FORCED SPATIAL VIBRATIONS OF A WOOD SHAPER CAUSED BY THE WEAR OF THE CUTTING TOOL

Georgi Vukov[1], Valentin Slavov[2], Pavlin Vichev[1], Zhivko Gochev[1]
[1]University of Forestry, Faculty of Forest Industry, Sofia, Bulgaria
[2]University of Chemical Technology and Metallurgy, Sofia, Bulgaria
e-mail: givukov@ltu.bg

ABSTRACT

This study presents the results of conducted investigations of the forced spatial vibrations of a wood shaper, caused by the wear of the cutting tool. The paper is based on a specific mechanical – mathematical model, developed by the authors, which allows studying of vibrations of this type of machinery. In this model the wood shaper is regarded as a system of three rigid bodies, which are connected by elastic and damping elements with each other and with the motionless floor. This study renders an account the mass, inertia, elastic and damping properties and geometric parameters of the machine. A necessary system of matrix differential equations is compiled and analytical solutions are presented. The results of the numerical investigations are presented. They are obtained through modern software and by using parameters of a particular machine. The results show that the amplitudes of the body's vibrations are relatively small but the amplitudes of the spindle's vibrations are significant especially at resonance zones.

Key words: forced spatial vibrations, cutting tool, woodworking shaper.

INTRODUCTION

The wear and damage of the cutting tools of the woodworking shapers inevitably affect the accuracy and quality of their production. There are some fixed regulations to their geometry, materials for production, ways of assembly of the cutting tool to the shaft and etc. (Gochev and Vukov 2017, Keturakis and Juodeikiene 2007, Prakasvudhisarn et al. 2009, Rousek et al. 2010). The practice in the exploitation of wood shapers indicates that one of the common problems in their use is the presence of unbalance (disbalance) of their cutting tools. The causes for rising of the unbalance may be occurrence of gaps, wrong or incorrect installation of the cutting tool on the shaft. But the main influence has uneven wear or damage of the tool and accumulation of superposition in separate parts of the instrument. The presence of unbalance of the cutting tool generates variable loads during the operation of the wood shapers. These loads are transmitted to the spindle and by its two bearing units reach the other elements and the machine's body and the driving electric motor. Specific studies for investigating the effect of the uneven wear and the damage of the cutting tool on the machine's work are required (Beljo-Lučić and Goglia, 2001; Orlowski et al., 2007). The machine can be seen as a mechanical vibrating system with known characteristics in these studies (Amirouche 2006; Coutinho 2010; Slavov and Vukov 2019).

The forced spatial vibrations of a woodworking shaper caused by the uneven wear and the damage of the cutting tool are investigated in the proposed study. It is assumed that they lead to an unbalance of the instrument but are not above the permissible limits. This research is aimed at the idle stroke of machine. It is a continuation of previous studies of the authors (Vukov et al. 2016, 2017, 2019). The vibrations on all 18 generalized coordinates of this mechanical system are investigated in this study.

MATHERIALS AND METHODS

A mechanic – mathematical model of woodworking shapers with lower spindle is built for studying its forced spatial vibrations. The model is shown in Figure 1.

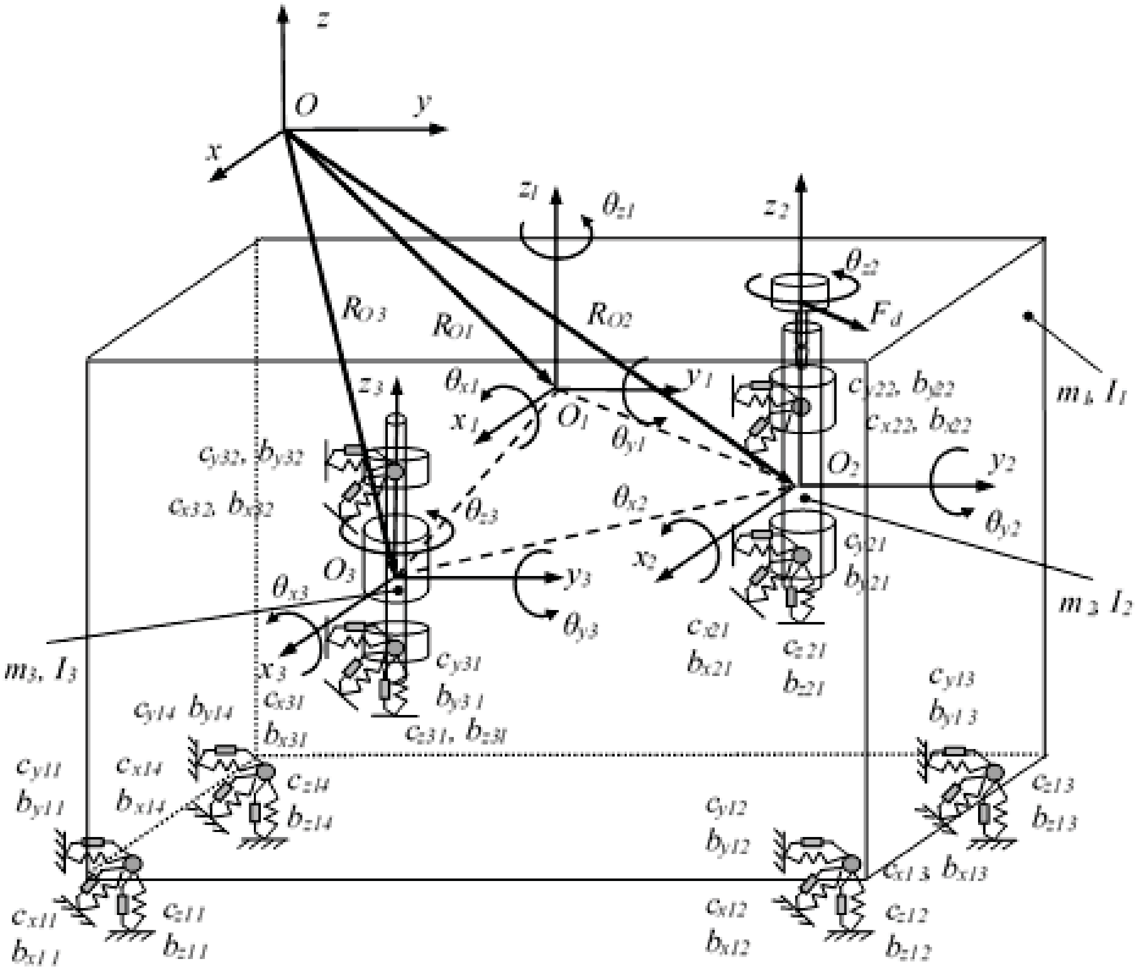

Figure 1: Mechanic-mathematical model of the wood shaper

The following symbols are used:

m_1, m_2, m_3 – mass of the shaper's body, the spindle and the rotor of the driving electric motor;

I_1, I_2, I_3 – inertia moment tensors of the woodworking shaper's body , the spindle and the rotor of the driving electric motor;

$c_{x1i}, c_{y1i}, c_{z1i}$, $i = 1, 2, 3, 4$– elastic coefficients of the vibroisolators between the machine's body and the floor;

$b_{x1i}, b_{y1i}, b_{z1i}$, $i = 1, 2, 3, 4$– damping coefficients of the vibroisolators between the machine's body and the floor;

$c_{x2i}, c_{y2i}, c_{z2i}$, $i = 1, 2$– elastic coefficients between the body of the machine and the spindle;

$b_{x2i}, b_{y2i}, b_{z2i}$, $i = 1, 2,$ – damping coefficients between the body of the machine and the spindle;

$c_{x3i}, c_{y3i}, c_{z3i}$, $i = 1, 2$– elastic coefficients between the body of the machine and the rotor of the driving electric motor;

$b_{x3i}, b_{y3i}, b_{z3i}$, $i = 1, 2,$ – damping coefficients between the body of the machine and the rotor of the driving electric motor.

The three bodies of the mechanical system perform spatial vibrations – three small translations and three small rotations relative to the axes of the rectangular local coordinate systems that are fixedly connected to the bodies. It is assumed that the axes of the local coordinate systems are parallel to the axes of the reference coordinate system. The position of the mechanical system in space is defined by the vector of the generalized coordinates, which is

$$\mathbf{q}=\left[x_1\ y_1\ z_1\ \theta_{x1}\ \theta_{y1}\ \theta_{z1}\ x_2\ y_2\ z_2\ \theta_{x_2}\ \theta_{y_2}\ \theta_{z_2}\ x_3\ y_3\ z_3\ \theta_{x3}\ \theta_{y3}\ \theta_{z3}\right]^{\mathrm{T}}. \tag{1}$$

The mechanical system has 18 degrees of freedom. The sequence of building of its mechanic-mathematical model is presented in previous works of the authors (Vukov et al. 2019). The free vibrations are investigated in these works. In this work, the model is further developed for the study of forced vibrations, caused by the wear and the damage of the cutting tool leading to its unbalance.

The differential equations of the forced spatial vibrations are derived by using the Lagrange's method.

$$\frac{d}{dt}\left(\frac{\partial E_K}{\partial \dot{q}}\right)-\left(\frac{\partial E_K}{\partial q}\right)+\frac{\partial F_b}{\partial \dot{q}}+\frac{\partial E_P}{\partial q}=\mathbf{Q} \tag{2}$$

where E_K and E_P are respectively the kinetic and the potential energy of the systems, and F_b is the dissipation energy or dissipative function. $\mathbf{Q}$ is the vector of generalized forces.

The obtained system of differential equations, which describes the forced spatial vibrations of the mechanical system, is

$$\mathbf{M}_{18\times18}.\ddot{\mathbf{q}}_{18\times1}+\mathbf{B}_{18\times18}.\dot{\mathbf{q}}_{18\times1}+\mathbf{C}_{18\times18}.\mathbf{q}_{18\times1}=\mathbf{Q}_{18\times1} \tag{3}$$

The matrix in these equations which characterizes the mass-inertial properties of the mechanical system is **M. B** is the matrix that characterizes the damping properties of this system and **C** – the elastic properties

The kinetic energy of the mechanical system is

$$E_K=\sum_{i=1}^{3}E_{K\,i}, \tag{4}$$

where $E_{Ki}=\frac{1}{2}.\left(\mathbf{m}_{\mathrm{RR}}^{\mathrm{i}}.\mathbf{V}_{\mathrm{Ci}}^{0\ \mathrm{T}}.\mathbf{V}_{\mathrm{Ci}}^{0}+\mathbf{\Omega}_{\mathbf{i}}^{\mathbf{i}\,\mathrm{T}}.\mathbf{I}_{\Theta\Theta}^{\mathrm{i}}.\mathbf{\Omega}_{\mathbf{i}}^{\mathbf{i}}\right)$, $\mathbf{m}_{\mathrm{RR}}^{\mathrm{i}}=\int_{V_i}\rho_i\ .\mathbf{I}\ .\mathrm{dV}_i=m_i.\mathbf{I}$.

The elements of the matrix **M** of mass-inertial properties are defined by the expression

$$m_{i,j}=\frac{\partial^2 E_K}{\partial\dot{q}_i.\partial\dot{q}_j} \tag{5}$$

Potential energy is defined by

$$E_P=E_{PK}(q)_k+E_{PG}(q)_i \tag{6}$$

where $E_{PK}(q)_m=\sum_{k=1}^{8}\frac{1}{2}.\mathbf{q}^{\mathrm{T}}.\mathbf{C}(\mathrm{q}).\mathbf{q}$,

$$E_{PG}(q)_i = \sum_{i=1}^{3} -m_i.\mathbf{g}^T.\mathbf{R}_{Ci}^0,$$

$\mathbf{C(q)}$ is a matrix of elastic properties;

$\mathbf{g} = \begin{bmatrix} 0 & 0 & g & 0 \end{bmatrix}^{\mathrm{T}}$ – vector of gravitational acceleration,

k is the number of the elastic element between two bodies of the mechanical system.

The elements of the matrix **C** of elastic properties are determined by the expression

$$c_{\mathrm{m,n}} = \frac{\partial^2 E_{PK}(q)_{ij}}{\partial q_n.\partial q_m} \quad (7)$$

Dissipative function is calculated by the formula

$$F_b = \sum \frac{1}{2}.b_k.\left(\boldsymbol{\delta}\dot{\mathbf{r}}_{\mathbf{k}}\right)^2 \quad (8)$$

where $\boldsymbol{\delta}\dot{\mathbf{r}}_{\mathbf{k}}$ is the deformation velocity of the elastic elements.

The elements of matrix **B** are obtained by replacing the elements of matrix **C** – $c_{i,j}$ with $b_{i,j}$.

The vector of the generalized external forces has the form

$$\mathbf{Q} = \begin{bmatrix} 0 & 0 & 0 & 0 & 0 & 0 & \mathbf{Q}_{\mathbf{F}(3\times1)}{}^{\mathrm{T}} & \mathbf{Q}_{\mathbf{Q}(3\times1)}{}^{\mathrm{T}} & 0 & 0 & 0 & 0 & 0 & 0 \end{bmatrix}^{\mathrm{T}} \quad (9)$$

$$\mathbf{Q}_{\mathbf{F}} = \begin{bmatrix} F_x \\ F_y \\ 0 \end{bmatrix}, \quad (10)$$

where $F_x = F_d.\cos(\omega t)$; $F_y = F_d.\sin(\omega t)$

$$\mathbf{Q}_{\mathbf{Q}}(F) = \mathbf{U}_{\mathbf{1}}^{\mathbf{\Omega 0}\mathrm{T}}.\left(\tilde{\mathbf{r}}_{\mathbf{P2}}^{\mathbf{0}\ \mathrm{T}}.\mathbf{Q}_{\mathbf{F}}\right), \quad (11)$$

where $\mathbf{U}_{\mathbf{1}}^{\mathbf{\Omega 0}\ \mathrm{T}} = \begin{bmatrix} 1 & 0 & \theta_{y1} \\ 0 & 1 & -\theta_{x1} \\ 0 & \theta_{x1} & 1 \end{bmatrix}^{\mathrm{T}}$; $\tilde{\mathbf{r}}_{\mathbf{P2}}^{\mathbf{0}\ \mathrm{T}} = \begin{bmatrix} 0 & l_{P2z}^0 & -l_{P2y}^0 \\ -l_{P2z}^0 & 0 & l_{P2x}^0 \\ l_{P2y}^0 & -l_{P2x}^0 & 0 \end{bmatrix}$;

$$\mathbf{r}_{\mathbf{P2}}^{\mathbf{0}} = \begin{bmatrix} l_{Px2}^0 \\ l_{Py2}^0 \\ l_{Pz2}^0 \end{bmatrix} = \begin{bmatrix} l_{x1}^0 + l_{x2}^1 + l_{Px2} \\ l_{y1}^0 + l_{y2}^1 + l_{Py2} \\ l_{z1}^0 + l_{z2}^1 + l_{Pz2} \end{bmatrix}; \quad \mathbf{r}_{\mathbf{P}2} = \begin{bmatrix} l_{Px2} \\ l_{Py2} \\ l_{Pz2} \end{bmatrix}.$$

Obtaining the common solutions of the system (3) is related to the determination of the initial conditions of movement $q(0)$ and $\dot{q}(0)$.

The general solutions of the system of differential equations in matrix form, with initial conditions $t=0,\ q(0)=q_0,\ \dot{q}(0)=\dot{q}_0$, are

$$q(t)=\sum_{r=1}^{18}\frac{2}{g_r^2+h_r^2}[\mathbf{G}_r.\mathbf{M}.\dot{q}(0)+(-\alpha_r.\mathbf{G}_r.\mathbf{M}+\beta_r.\mathbf{H}_r.\mathbf{M}\quad+\mathbf{G}_r.\mathbf{B}).q(0)].e^{-\alpha_r t}.\cos\beta_r t+$$
$$+\sum_{r=1}^{18}\frac{2}{g_r^2+h_r^2}[\mathbf{H}_r.\mathbf{M}.\dot{q}(0)+(-\alpha_r.\mathbf{H}_r.\mathbf{M}-\beta_r.\mathbf{G}_r.\mathbf{M}+\mathbf{H}_r.\mathbf{B}).q(0)].e^{-\alpha_r t}.\sin\beta_r t+$$
$$+\mathrm{Re}\{\sum_{k=0}^{n}\sum_{r=1}^{18}\frac{2}{g_r^2+h_r^2}.\frac{\alpha_r.\mathbf{G}_r+\beta_r.\mathbf{H}_r+i.k.\Omega.\mathbf{G}_r}{\omega_r^2-k^2.\Omega^2+i.2.k.\sigma_r.\omega_r.\Omega}\mathbf{Q}.e^{ik\Omega t}\} \quad \mathbf{(12)}$$

where

$$g_r=-2.\alpha_r\left(\mathbf{V}_r^{\mathrm{T}}.\mathbf{M}.\mathbf{V}_r-\mathbf{W}_r^{\mathrm{T}}.\mathbf{M}.\mathbf{W}_r\right)-4.\beta_r.\mathbf{V}_r^{\mathrm{T}}.\mathbf{M}.\mathbf{W}_r+\mathbf{V}_r^{\mathrm{T}}.\mathbf{B}.\mathbf{V}_r-\mathbf{W}_r^{\mathrm{T}}.\mathbf{B}.\mathbf{W}_r;$$
$$h_r=2.\beta_r\left(\mathbf{V}_r^{\mathrm{T}}.\mathbf{M}.\mathbf{V}_r-\mathbf{W}_r^{\mathrm{T}}.\mathbf{M}.\mathbf{W}_r\right)-4.\alpha_r.\mathbf{V}_r^{\mathrm{T}}.\mathbf{M}.\mathbf{W}_r+2.\mathbf{V}_r^{\mathrm{T}}.\mathbf{B}.\mathbf{W}_r;$$
$$\mathbf{G}_r=g_r.\mathbf{L}_r+h_r.\mathbf{R}_r;\quad \mathbf{L}_r=\mathbf{V}_r.\mathbf{V}_r^{\mathrm{T}}-\mathbf{W}_r.\mathbf{W}_r^{\mathrm{T}};$$
$$\mathbf{H}_r=h_r.\mathbf{L}_r-g_r.\mathbf{R}_r;\quad \mathbf{R}_r=\mathbf{V}_r.\mathbf{W}_r^{\mathrm{T}}+\mathbf{W}_r.\mathbf{V}_r^{\mathrm{T}}. \quad \mathbf{(13)}$$

The whole machine and the three bodies are modelled with software Solid Works. These models are shown respectively in Figure 2, Figure 3, Figure 4 and Figure 5. Figure 2 shows the local coordinate systems and the reference coordinate system that coincides with the coordinate system of the body 1 and in which all the vectors are projected. It is assumed that the axes of the local coordinate systems are parallel to the axes of the reference coordinate system. The elastic-damping elements are marked with points 1 to 8. The application point of the disturbing force F_d, which coincides with the mass center of the tool, is marked by point 9.

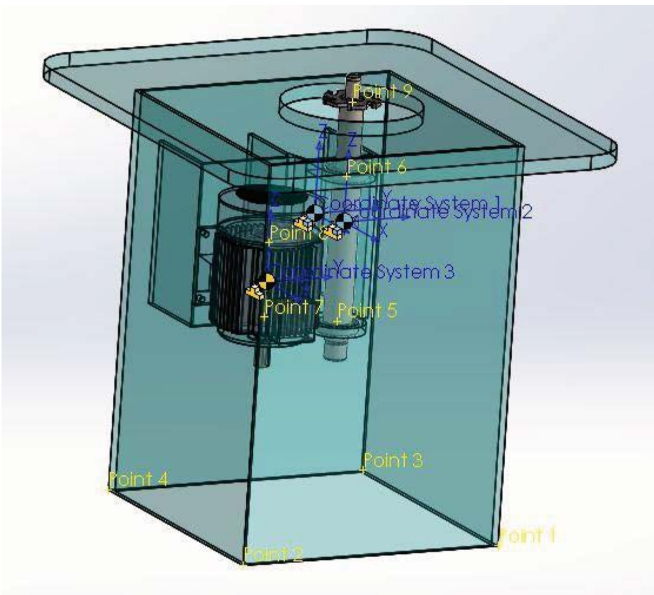

Figure 2: Model of the whole *machine*

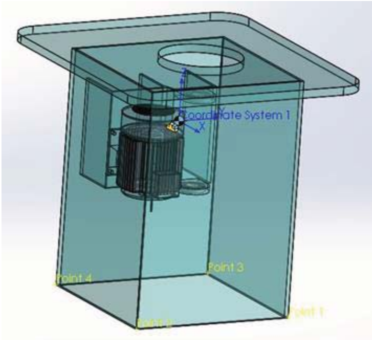

Figure 3: Model of body1

Figure 4: Model of body2

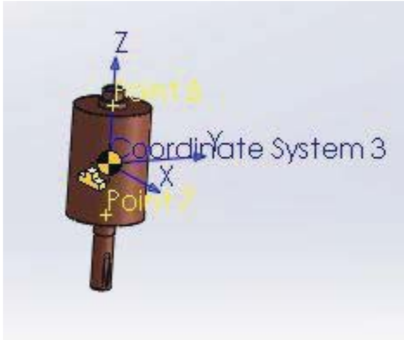

Figure 5: Model of body3

Table 1: Technical characteristics of the machine

Body №	Mass, *kg*	Mass inertia moments, *kg.m²*						Coordinates of the mass centers, *m*		
	m	J_{xx}	J_{yy}	J_{zz}	J_{xy}	J_{yz}	J_{xz}	l_{Cx}	l_{Cy}	l_{Cz}
1	391,52	49,2672	52,0000	47,9480	0,0395	0,4405	0,2525	0	0	0
2	11,123	0,2937	0,2937	0,0052	0	0	0	0,009	0,066	-0,020
3	14,378	0,0516	0,0516	0,0206	0	0	0	0,019	-0,115	-0,134

Coordinates of the supporting points of the elastic and damping elements

In the coordinate system of the body 1				**In the coordinate system of the body 2**			
т.	l_{xi}, m	l_{yi}, m	l_{zi}, m	т.	l_{xi}, m	l_{yi}, m	l_{zi}, m
1	0,309	0,316	-0,654	5	0	0	-0,214
2	0,309	-0,284	-0,654	6	0	0	0,096
3	-0,291	0,316	-0,654	9	-0,005	0,005	0,258
4	-0,291	-0,284	-0,654				
In the coordinate system of the body 3				**In the coordinate system of the body 1**			
т.	l_{xi}, m	l_{yi}, m	l_{zi}, m	т.	l_{xi}, m	l_{yi}, m	l_{zi}, m
7	0	0	-0,076	5	0,009	0,066	-0,234
8	0	0	0,084	6	0,009	0,066	0,076
				7	0,019	-0,015	-0,210
				8	0,019	-0,015	-0,050

Damping coefficients

Between Bodies	b_{xi}, (N.s)/m	b_{yi}, (N.s)/m	b_{zi}, (N.s)/m
0 and 1	980	670	470
1 and 2	980	670	470
1 and 3	980	670	470

Elasticity coefficients

Between Bodies	c_{xi}, N/m	c_{yi}, N/m	c_{zi}, N/m
0 and 1	1000000	1000000	1500000
1 and 2	2250000	2250000	2250000
1 and 3	2250000	2250000	2250000

Disturbing forces: F_d = 19,62 N; F_d = 29,44 N; F_d = 39,24 N

Rotational frequency: 100 s^{-1} = 15,9 Hz.

RESULTS AND DISCUSSION

The vibrations on all 18 generalized coordinates of this mechanical system are obtained as a result of the provided investigations. Due to the limited volume of the article, only a few of them are illustrated here. The linear vibrations on the three coordinates of the machine's body, the rotor of the electric motor and the spindle are presented. The results are given at rotational frequency 100 s^{-1} and disturbing force F_d = 19,62 N; F_d = 29,44 N; F_d = 39,24 N. The amplitudes of the considered coordinates are presented on the next figures

I. F_d = 19,62 N

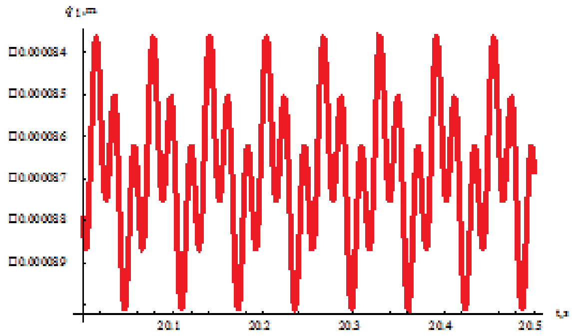

Figure 6: Graph of $q_1(x_1)$

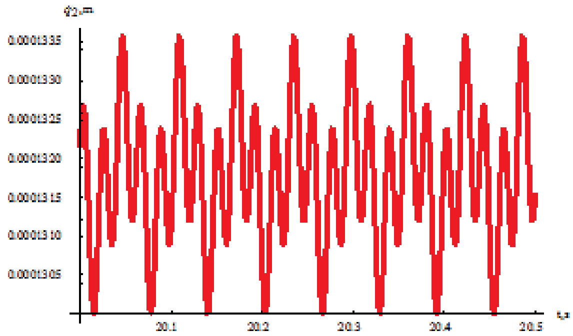

Figure 7: Graph of $q_2(y_1)$

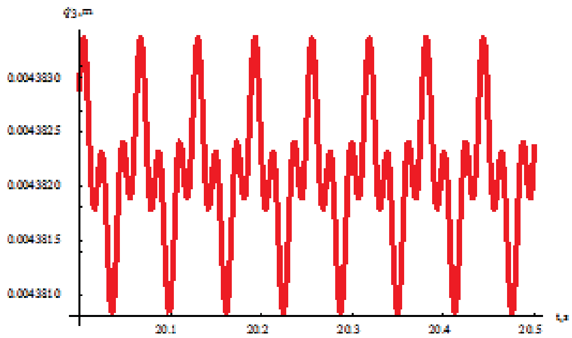

Figure 8: Graph of $q_3(z_1)$

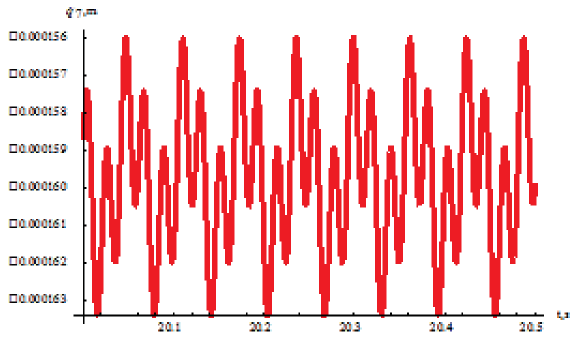

Figure 9: Graph of $q_7(x_2)$

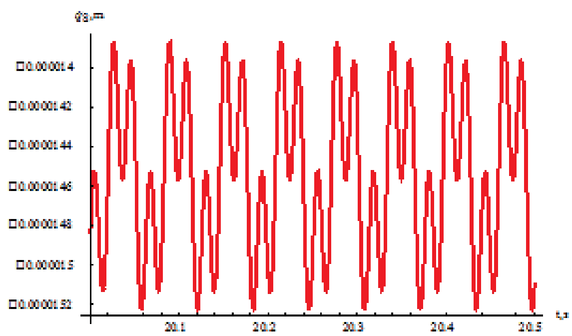

Figure 10: Graph of $q_8(y_2)$

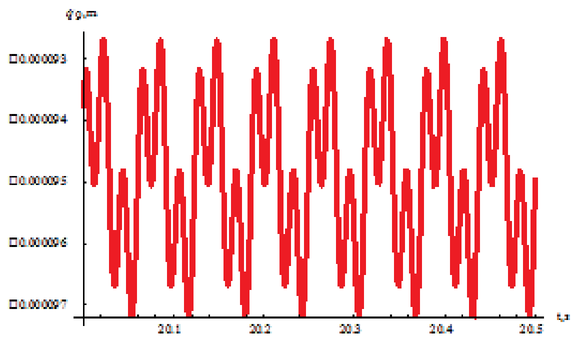

Figure 11: Graph of q9(z2)

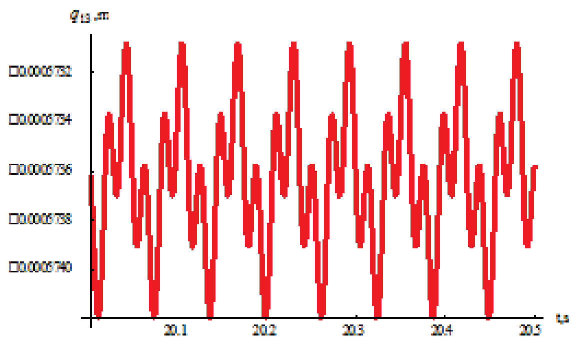

Figure 12: Graph of $q_{13}(x_3)$

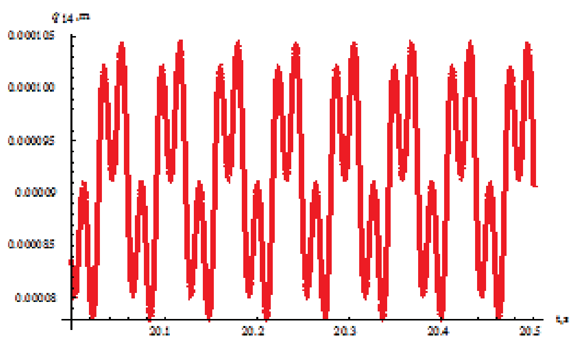

Figure 13: Graph of $q_{14}(y_3)$

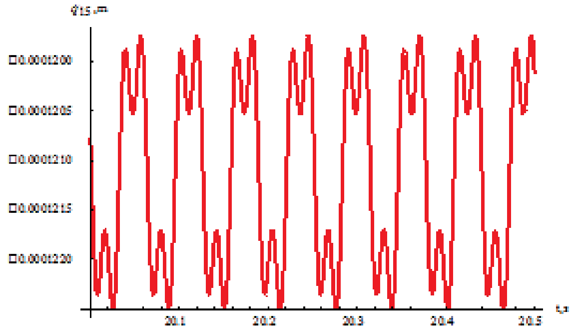

Figure 14: Graph of $q_{15}(z_3)$

II. F_d = 29,44 N

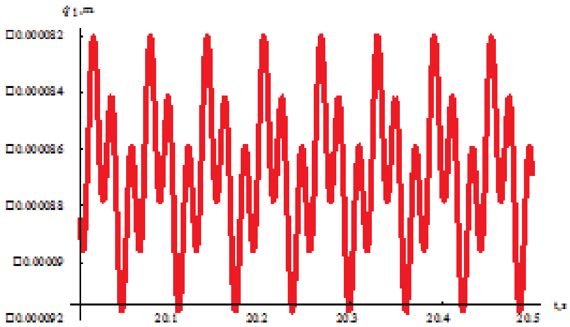

Figure 15: Graph of $q_1(x_1)$

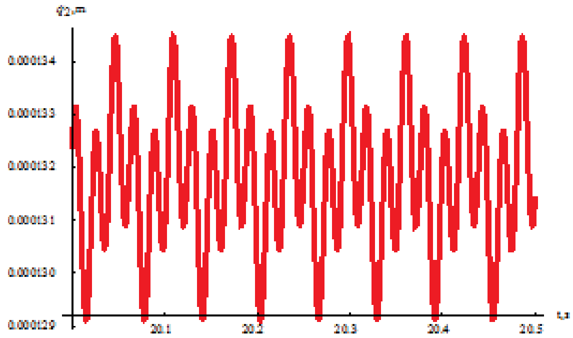

Figure 16: Graph of $q_2(y_1)$

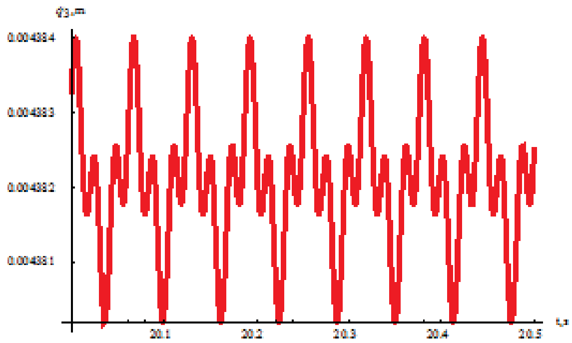

Figure 17: Graph of $q_3(z_1)$

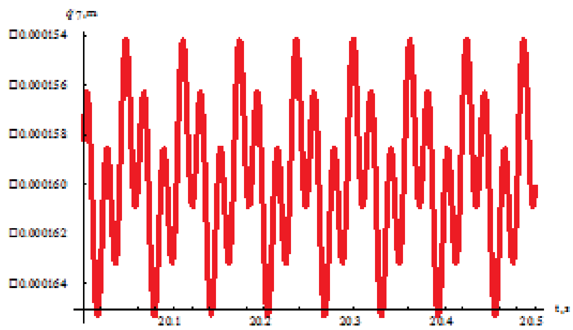

Figure 18: Graph of $q_7(x_2)$

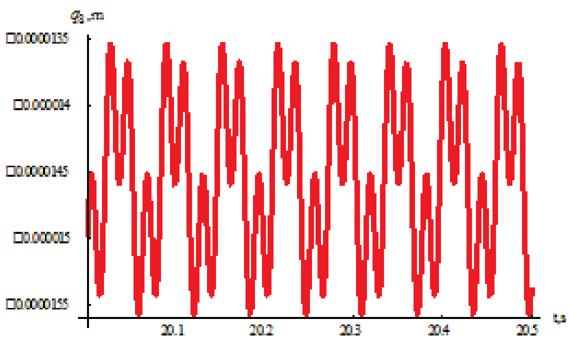

Figure 19: Graph of $q_8(y_2)$

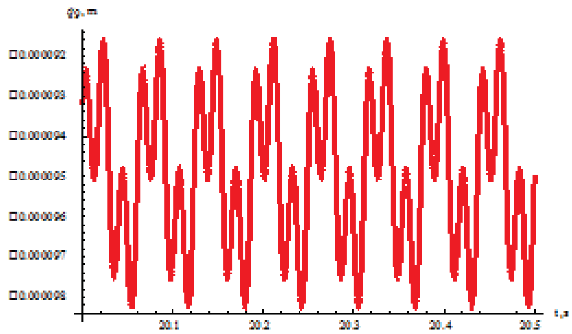

Figure 20: Graph of $q_9(z_2)$

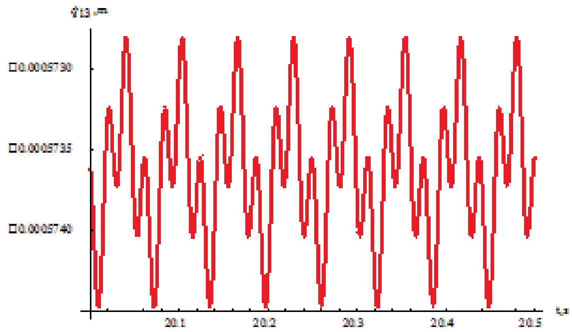

Figure 21: Graph of $q_{13}(x_3)$

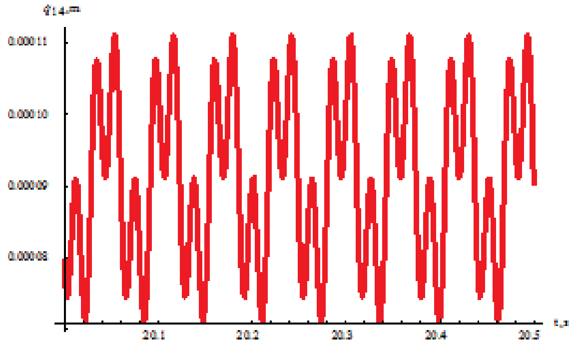

Figure 22: Graph of $q_{14}(y_3)$

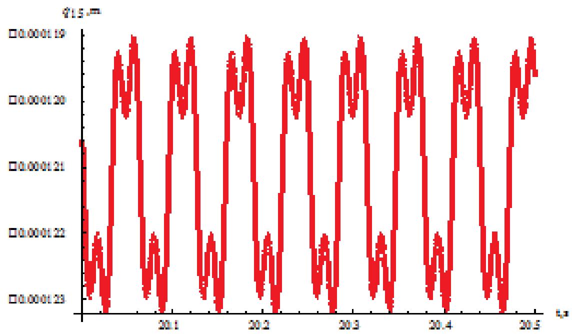

Figure 23: Graph of $q_{15}(z_3)$

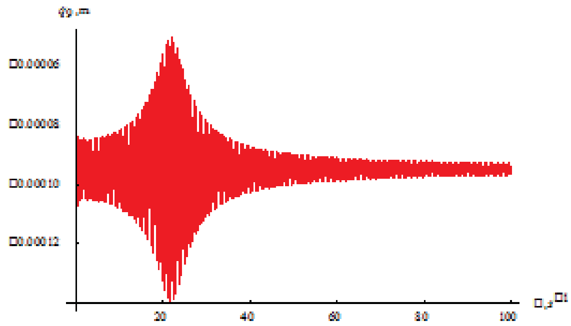

III. F_d = 39,24 N

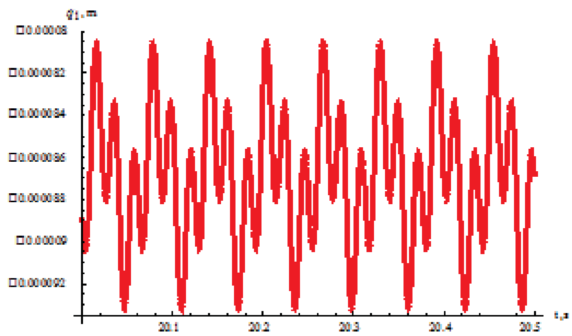

Figure 24: Graph of $q_1(x_1)$

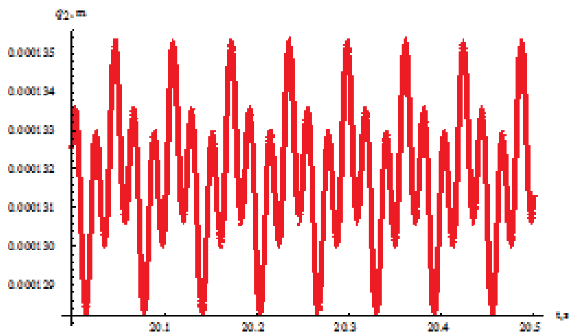

Figure 25: Graph of $q_2(y_1)$

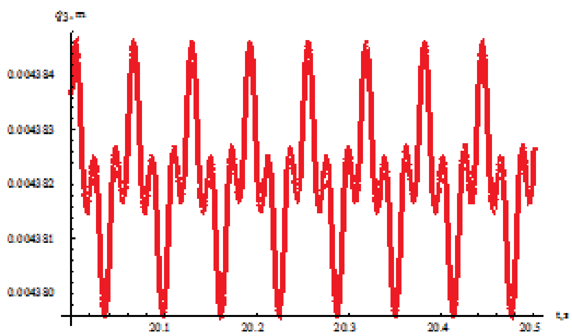

Figure 26: Graph of $q_3(z_1)$

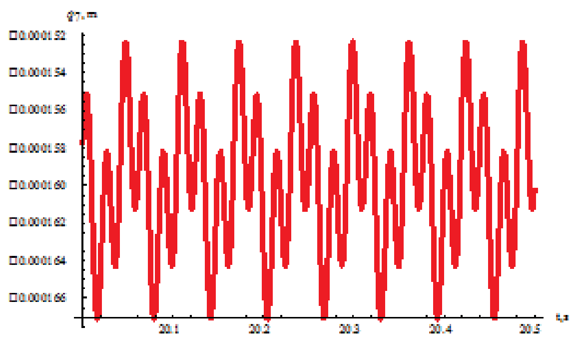

Figure 27: Graph of $q_7(x_2)$

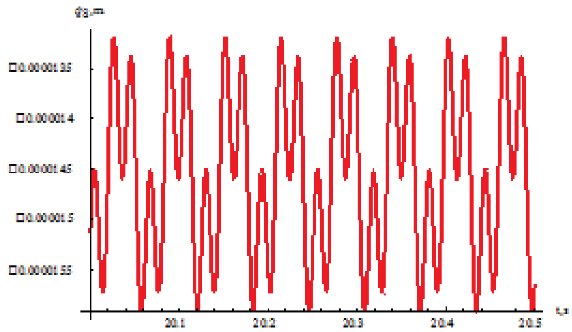

Figure 28: Graph of *$q_8(y_2)$*

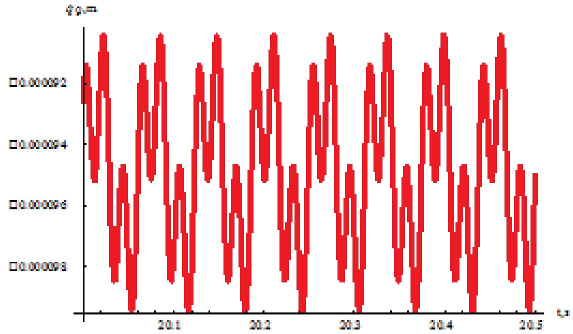

Figure 29: Graph of *$q_9(z_2)$*

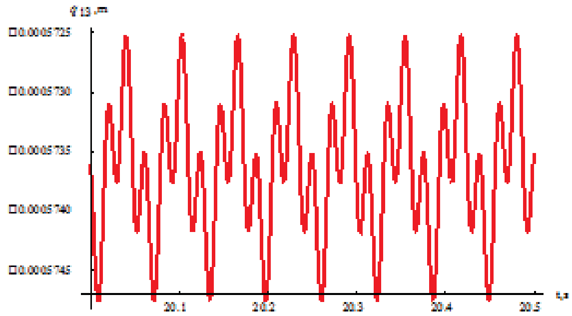

Figure 30: Graph of *$q_{13}(x_3)$*

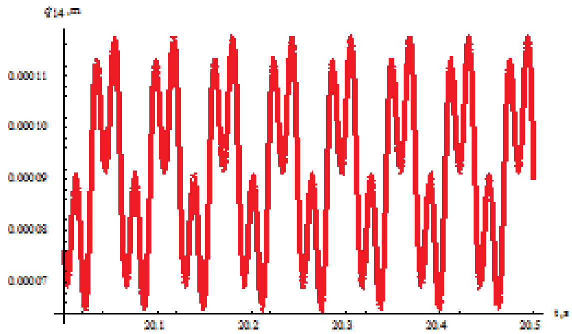

Figure 31: Graph of *$q_{14}(y_3)$*

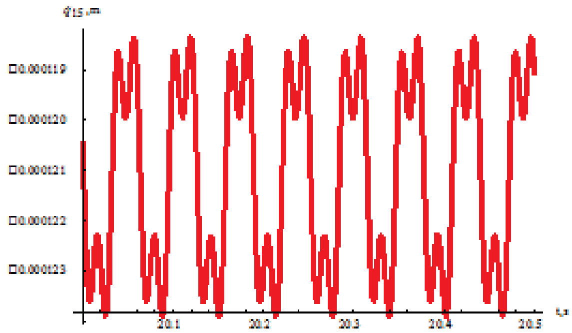

Figure 32: Graph of *$q_{15}(z_3)$*

Maximum amplitude on coordinate z_2 at circular frequency 20,3 s^{-1} – 0,1 mm

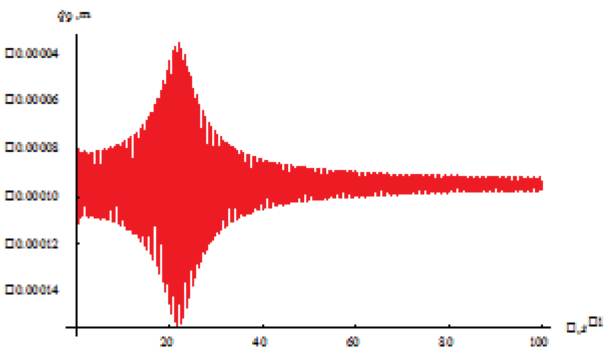

Figure 33: Graph of *$q_9(z_2)$*

Some conclusions can be drawn from the presented graphs. The amplitudes of the body's vibrations on the three coordinates are relatively small. The amplitudes of the spindle's vibrations on the coordinates x_2 and y_2 are small, but the amplitude on the coordinate z_2 at a frequency of 20,3 s^{-1} (at resonance) is greater (0.1 mm). These vibrations have little effect on the interaction between the cutting tool and processed material by their own but at resonance their effect is significant. The vibration's amplitudes of the cutting tool, which does not exceed the permissible limits leading to the unbalance under consideration, do not significantly affect the normal operation of the machine.

CONCLUSIONS

The paper presents a study of the forced spatial vibrations of a woodworking shaper. These vibrations are caused by uneven wear and damage of the cutting tool. This work assumes that they lead to an unbalance of the tool which is not above the permissible limits. Some numerical calculations are carried out with a developed machine's model and modern computer programs. The calculations use the parameters of a woodworking machine used in the practice. The vibrations of the mechanical system on all the 18 generalized coordinates are obtained as a result of these investigations. The results are analyzed and conclusions are drawn for the vibrations amplitudes by the individual coordinates for each of these bodies at the considered unbalance. As a result of the study, the impact of the tool's unbalance on the operation of the main elements of the machine is clarified. Investigated vibrations have significant effect on the interaction between the cutting tool and processed material at resonance zones. The obtained results concern mainly the idle stroke of machine. The next part of this paper examines the effect of tool wear on the vibration of the machine, again taking into account its imbalance but also the change in cutting forces when it interacts with the processed material.

ACKNOWLEDGEMENTS

This paper is supported by the Scientific Research sector at the University of Forestry, Sofia, Bulgaria, under contract No SRS-B-1012/27.03.2019

REFERENCES

AMIROUCHE F. 2006. Fundamentals of Multibody Dynamics – Theory and Applications. Birkhäuser, Boston, 345 p.

BELJO-LUČIĆ R, GOGLIA V. 2001. Some possibilities for reducing circular saw idling noise. Journal of Wood Science, 47(5): pp. 389–393,

COUTINHO M. 2010. Dynamic Simulations of Multibody Systems, Springer-Verlag, New-York.

FILIPOV G. 1977. Woodworking machines. Sofia, 345 p. (in Bulgarian)

GOCHEV ZH., VUKOV G. 2017. Influence of the Wearing of the Saw Unit Elements of the Wood Shaper on the System Vibration. Acta Facultatis Xylologiae Zvolen, 59(2): pp. 147−153.

GRIGOROV P. 1985. Cutting of wood (in Bulgarian). Technics. Sofia.

KETURAKIS G., JUODEIKIENE I. 2007. Investigation of Milled Wood Surface Roughness. Materials science 13(1): pp. 47–51.

ORLOWSKI K., SANDAK J., TANAKA C. 2007. The critical rotational speed of circular saw: simple measurement method and its practical implementations. Journal of Wood Science, 53(5): pp. 388–393.

PRAKASVUDHISARN C., KUNNAPAPDEELERT S.; YENRADEE P. 2009. Optimal cutting condition determination for desired surface roughness in end milling. The International Journal of Advanced Manufacturing Technology, 41: pp. 440–451.

ROUSEK M., KOPECKÝ Z., SVATOŠ M. 2010. Problems of the quality of wood machining by milling stressing the effect of parameters of machining on the kind of wood. Annals of Warsaw University of Life Sciences – SGGW 72 No 72: pp. 233–242.

SLAVOV V., VUKOV G. 2019. Modelling and researching of forced spatial vibrations of axial fans. MATEC Web of Conferences V.287, a.№ 03006.

VUKOV, G., ZH. GOCHEV, V. SLAVOV, P. VICHEV, V. ATANASOV. 2016. Mechanic-Mathematical Model for Investigations of the Natural Frequencies and Mode Shapes of the Free Spatial Vibrations of Wood Shaper and its Spindle, Proceedings of the 10th International Science Conference „Chip and Chipless Woodworking Processes", Zvolen, 10(1), pp. 203–209.

VUKOV G., ZH. GOCHEV, V. SLAVOV, P. VITCHEV, V. ATANASOV. 2017. Numerical Investigations of the Forced Spatial Vibrations of Wood Shaper and its Spindle, Caused by Unbalance of the Cutting Tool, PRO LIGNO, Transilvania University Press Brasov, Romania, Vol. 13, №4, pp. 154–161.

VUKOV G., V. SLAVOV, P. VICHEV, ZH. GOCHEV. 2019. Investigations of the Free Space Vibrations of a Woodworking Shaper, Considered as a Mechanical System with Three Main Bodies, Proceedings 4th International Scientific Conference ”WOOD TECHNOLOGY & PRODUCT DESIGN”, Ohrid, Republic of Macedonia, pp. 127–135.

VUKOV G., P. VICHEV, V. SLAVOV, ZH. GOCHEV. 2019. Free Damped Space Vibrations of a Woodworking Shaper, Considered as a mechanical system with three main bodies, Proceedings 4th International Scientific Conference ”WOOD TECHNOLOGY & PRODUCT DESIGN”, Ohrid, Republic of Macedonia, pp. 136–145.

UNIVERSITY OF FORESTRY

FACULTY OF FOREST INDUSTRY

INNOVATION IN WOODWORKING INDUSTRY AND ENGINEERING DESIGN

2/2021

INNO vol. X Sofia

ISSN 1314-6149
e-ISSN 2367-6663

Indexed with and included in CABI

INNOVATION IN WOODWORKING INDUSTRY AND ENGINEERING DESIGN

Science Journal
Vol. 10/p. 1–90
Sofia 2/2021

ISSN 1314-6149
e-ISSN 2367-6663

Edition of
FACULTY OF FOREST INDUSTRY – UNIVERSITY OF FORESTRY – SOFIA

The Scientific Journal is indexed with and included in CABI.

Cover Design: DESISLAVA ANGELOVA

Printed by: INTEL ENTRANCE
Publisher address: UNIVERSITY OF FORESTRY – FACULTY OF FOREST INDUSTRY
Kliment Ohridski Bul., 10, Sofia, 1797, BULGARIA
http://inno.ltu.bg
http://www.scjournal-inno.com/

CONTENTS